EARTHQUAKE ENGINEERING AND STRUCTURAL DYNAMICS, VOL. 25, 611–629 (1996)

EQUIVALENT LINEARIZATION OF GENERALLY PINCHING HYSTERETIC, DEGRADING SYSTEMS

GREG C. FOLIENTE*
CSIRO Division of Building, Construction and Engineering, P.O. Box 56, Highett, Victoria 3190, Australia

MAHENDRA P. SINGH†
Department of Engineering Science and Mechanics, Virginia Polytechnic Institute and State University, Blacksburg, VA 24061-0219, U.S.A.

AND

MOHAMMAD N. NOORI‡
Mechanical Engineering Department, Worcester Polytechnic Institute, Worcester, MA 01609-2280, U.S.A.

SUMMARY

Many types of structural systems that undergo cycles of inelastic deformation under severe natural hazard loadings exhibit 'pinching' of hysteresis loops. In this paper, a generally pinching hysteretic restoring force model—an extension of the Bouc–Wen differential hysteresis model—is used in stochastic equivalent linearization of single-degree-of-freedom structural systems. The severity and rate of pinching are controlled by the hysteretic energy dissipation and the pinching level can be specified to match experimental data. Under white noise excitations, estimates of reponse statistics from linearization are shown to compare favourably with those from Monte Carlo simulation. Numerical studies on the sensitivity of the accuracy of response statistics obtained by linearization to changes in the hysteresis parameters showed that, for a range of practical cases, the linearization method can be used in lieu of simulation and that, in low-frequency systems, some hysteresis parameters may be set to a constant value *a priori* to reduce the number of model parameters that needs to be estimated or identified, and to simplify further random vibration analysis and/or performance evaluation studies.

KEY WORDS: equivalent/statistical linearization; hysteretic systems; random vibrations; stochastic dynamic analysis

1. INTRODUCTION

Most structures undergo cycles of inelastic deformation under severe natural hazard dynamic loads, such as strong ground motion, extreme wind and wave action. Random vibration techniques provide a rational way to calculate structural response to natural hazard loadings modelled as random processes. In non-linear random vibrations, an exact solution is severely limited to a few systems, but developments in approximate solution techniques and their application to practical engineering problems have accelerated in the last three decades. A significant contribution in this area was Wen's[1,2] and Baber and Wen's[3] modification of Bouc's[4] smoothly varying hysteresis model, and stochastic equivalent linearization of the resulting model without recourse to the Krylov–Bogoliubov approximation based on a direct linearization scheme.[5] Because of the versatility and mathematical tractability of the Bouc–Wen model, it quickly gained popularity and has, since then, been extended and applied to a wide variety of engineering problems,[6,7] including multi-degree-of-

*Senior Research Scientist
†Professor
‡Professor and Head

CCC 0098-8847/96/060611-19

Received 29 January 1995
Revised 15 December 1995

freedom (MDOF) shear buildings[2,8] and frames,[9-12] bidirectional and torsional response of hysteretic systems,[13-15] two- and three-dimensional continua,[16,17] soil liquefaction,[18] and base isolation systems,[19] among many others. The Bouc–Wen model and its variants/extensions have been used in the modelling and analysis of structures built of reinforced concrete,[20,21] steel,[20,22] masonry[23] and timber.[24] Recognizing the increasing importance of using the Bouc–Wen model in nonlinear dynamic analysis, Wong *et al.*[25,26] studied the multiharmonic steady-state responses of a single-degree-of-freedom (SDOF) Bouc–Wen oscillator under periodic excitations, and performed a detailed and systematic study of the influence of the parameters of the original Bouc–Wen model on steady-state responses and hysteresis loops.

Among the currently available methods of non-linear random vibrations, the equivalent linearization method is the most useful for practical engineering applications, especially for systems of high dimensionality and high non-linearity. Wen[2] used this method in computing the stochastic dynamic response of the original Bouc–Wen oscillator. The theory and applications of the equivalent linearization method in random vibration problems have been synthesized.[27] Despite its inherent limitation of only yielding estimates of the first and second moments of the response, and the assumption of Gaussian response (which means that it may not accurately reflect the effects of non-linearities on the distribution of the response), linearization remains a very useful and practical method in the first stage of design—that is, when an optimal system is sought and 'the influence of various disposable system parameters on the overall level of response'[27] is studied. To obtain better response estimates, some researchers have proposed alternative linearization schemes[28-30] or an error-correction scheme.[31] Response statistics of the Bouc–Wen oscillator have also been obtained using various approximate methods—such as numerical solution of the Fokker–Planck–Kolmogorov (FPK) diffusion equation,[32] FPK with a cumulant truncation technique,[33] cumulant neglect closure,[34,35] stochastic averaging,[36] path integral solution technique[37] and a method based on balancing the average energy dissipation.[38]

Realistic modelling of natural hazard loadings by random processes and improved solution procedures should not be counterbalanced, however, by limited hysteresis models. The basic Bouc–Wen model is versatile but it did not originally model the pinching and degradation behaviour exhibited by many hysteretic systems. Since degradation can lead to progressive damage and/or total collapse, the model was extended to allow strength and/or stiffness degradation.[3] Sues *et al.*[39] proposed an alternative stiffness degradation scheme that can be used for reinforced concrete structures. Casciati[40] added two terms to the hysteretic constitutive equation to minimize artificial drift when the (cyclic) loading does not change sign. An alternative way to reduce the local violation of Drucker's stability postulate of plasticity when the system undergoes intermediate loading–reloading has been proposed.[26] To model the observed pinching behaviour of some reinforced concrete and steel structures, further extensions to the model have been presented.[41-44] The resulting degrading, pinching model with the extensions proposed by Baber and Wen,[3] and Baber and Noori[43] will be called herein the Bouc–Wen–Baber–Noori (BWBN) model. This model, however, forces pinching to occur when the load changes sign (i.e. at zero load). Experimental hysteresis plots of various structural systems (Figure 1) show that pinching occurs at some residual force level. Thus, the BWBN restoring force model should be generalized further to model this off-the-origin pinching effect. Although Pradlwarter and Schuëller[30] have presented a powerful linearization technique for MDOF systems with *any* empirically derived hysteresis models, including those with complex force-history rules, there are certain advantages in using a general mathematical constitutive relation as provided by the BWBN model.

This paper presents an equivalent linearization procedure for hysteretic structural systems with general pinching behaviour (Figure 1), modelled by an extension of the BWBN model which allows control of the off-the-origin pinching effect. For simplicity, the present work is limited to the zero-mean random vibration analysis of SDOF systems. The procedure, however, is general and may be used to study the stochastic dynamic response of various kinds of multi-degree-of-freedom structural systems [e.g., steel, reinforced concrete, timber (Figure 1) using shear beam or discrete hinge structural models] as long as appropriate hysteresis model parameters for these systems are known. Sensitivity of the accuracy of response statistics estimates to changes in the hysteresis parameters is also studied in the present work.

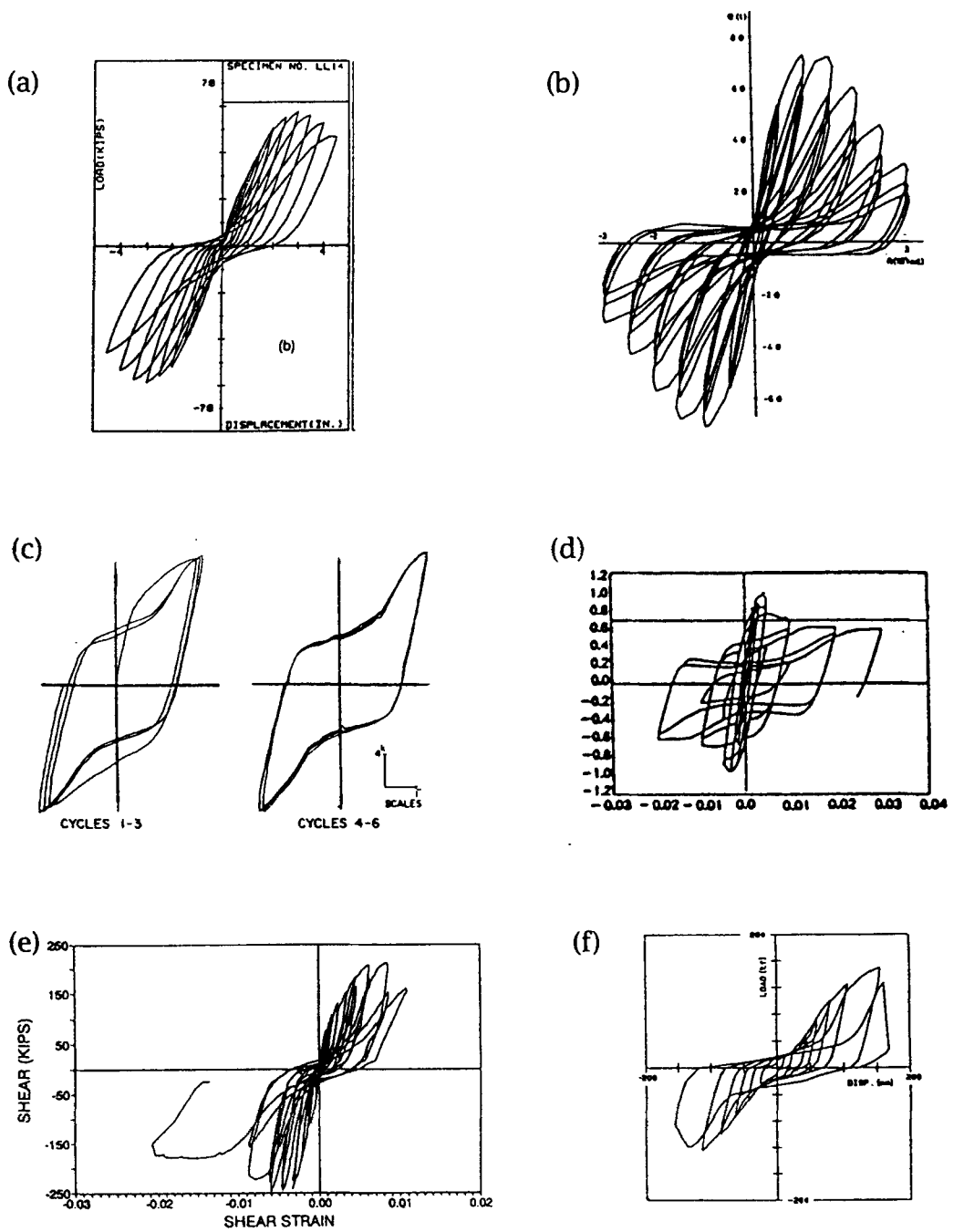

Figure 1. Pinching, degrading hysteretic systems: (a) high-strength RC connection (from Reference 45); (b) RC beam-and-column connection (from Reference 46); (c) steel beam-and-column connection (from Reference 47); (d) X-braced steel frame (from Reference 48); (e) reinforced gypsum-roof diaphragm (from Reference 49); (f) braced glulam timber frame (from Reference 50)

2. RESTORING FORCE MODEL

The equation of motion of the non-linear SDOF system shown in Figure 2, in standard form, is

$$\ddot{u} + 2\xi_0\omega_0\dot{u} + \alpha\omega_0^2 u + (1-\alpha)\omega_0^2 z = f(t) \tag{1}$$

where u is the relative displacement of the mass with respect to the ground (dots designate derivatives with respect to time t), ξ_0 is the system damping ratio, ω_0 is the system's linear natural frequency, $f(t)$ is the mass-normalized forcing function (assumed zero-mean), α is the ratio of post-yielding to pre-yielding stiffness (or rigidity ratio) and z is the hysteretic displacement. The constitutive law is given by the following first-order non-linear differential equation:

$$\dot{z} = h(z)\left\{\frac{\dot{u} - v(\beta|\dot{u}||z|^{n-1}z + \gamma\dot{u}|z|^n)}{\eta}\right\} \tag{2}$$

where β, γ, n are the hysteresis shape parameters (if $n = \infty$, the elastoplastic hysteresis case is obtained), v, η are the strength and the stiffness degradation parameters, respectively (if $v = \eta = 1{\cdot}0$, the model does not degrade), and $h(z)$ is the pinching function[24] [if $h(z) = 1{\cdot}0$, the model does not pinch]. The properties and details of the non-pinching model can be found in References 1, 3 and 26 and those of the pinching model in References 24, 41 and 43. (Note that the hysteresis shape parameter A in the original Bouc–Wen model has been set to unity.) Different values of β and γ give various softening and hardening systems. The hysteretic restoring force is given by the fourth term in equation (1) as $(1-\alpha)\omega_0^2 z$. Since $[(1-\alpha)\omega_0^2]$ is assumed as a time-invariant system property, the hysteretic restoring force will also be referred to as z from hereon. The hereditary restoring force model implies that the response is completely specified by the differential equation given a displacement time history. The functions that define v, η and $h(z)$ are given in Appendix I.

Pinching is primarily caused by damage and interaction of structural components under large deformation. It is caused by 'closing (or unclosed) cracks and yielding of compression reinforcement before closing of the cracks[51]' in reinforced concrete members, slipping at bolted joints in steel construction, and loosening and slipping of the joints caused by previous cyclic loadings in timber structures with dowel-type fasteners,[24] e.g. nails and bolts. In steel and timber systems, the hysteresis trace recovers from the pinching effect and shows stiffening when bearing on the dowel-type fastener is initiated.

Noori[41] proposed three possible pinching models: two of the models are series models consisting of the Bouc–Wen smooth hysteresis model with slip lock elements[42] and one is a single-element pinching model.[43] The three models were used in zero and non-zero mean random vibration analysis.

The generalized pinching model used herein, completely described by equations (1), (2) and equations (17)–(21) in Appendix I, and called the *modified* BWBN model, is very versatile and can account for the hysteretic behaviour of many structural systems (e.g. Figure 1). Its general pinching capability under deterministic cyclic loading has been verified for timber structural systems[24, 52] but this capability would be equally valid for other structures; the pinching level can be varied to match experimental data. If $h(z)$ is set to

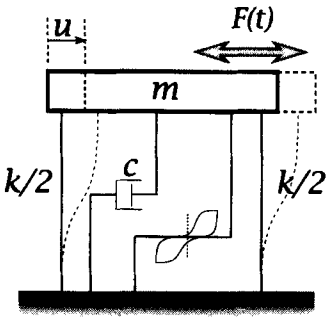

Figure 2. Single-degree-of-freedom oscillator

unity, the degrading Bouc–Wen model is obtained. If $h(z)$ is set to unity, and δ_ν and δ_η are set to zero, the original Bouc–Wen model is obtained.

Sample hysteresis plots of SDOF systems under Gaussian white noise excitation with power spectral density $S_0 = 1{\cdot}0$ are shown in Figure 3. Both systems have $\omega_0 = 2{\cdot}0$ rad/s, $\xi_0 = 0{\cdot}05$, $\alpha = 0{\cdot}10$, $\beta = 1{\cdot}5$, $\gamma = -0{\cdot}5$, $n = 1$, $q = 0{\cdot}10$, $\lambda = 0{\cdot}05$, $p = 1$, $\psi_0 = 0{\cdot}20$ and $\delta_\psi = 0{\cdot}002$ (see Appendix I for definitions). Figure 3(a) is a non-degrading, low pinching system with $\zeta_{1_0} = 0{\cdot}85$ and $\delta_\eta = \delta_\nu = 0{\cdot}0$, while Figure 3(b) is a degrading, high pinching system with $\zeta_{1_0} = 0{\cdot}97$, $\delta_\nu = 0{\cdot}005$ and $\delta_\eta = 0{\cdot}05$. It is seen that a larger value of ζ_{1_0} produces a more severe pinching.

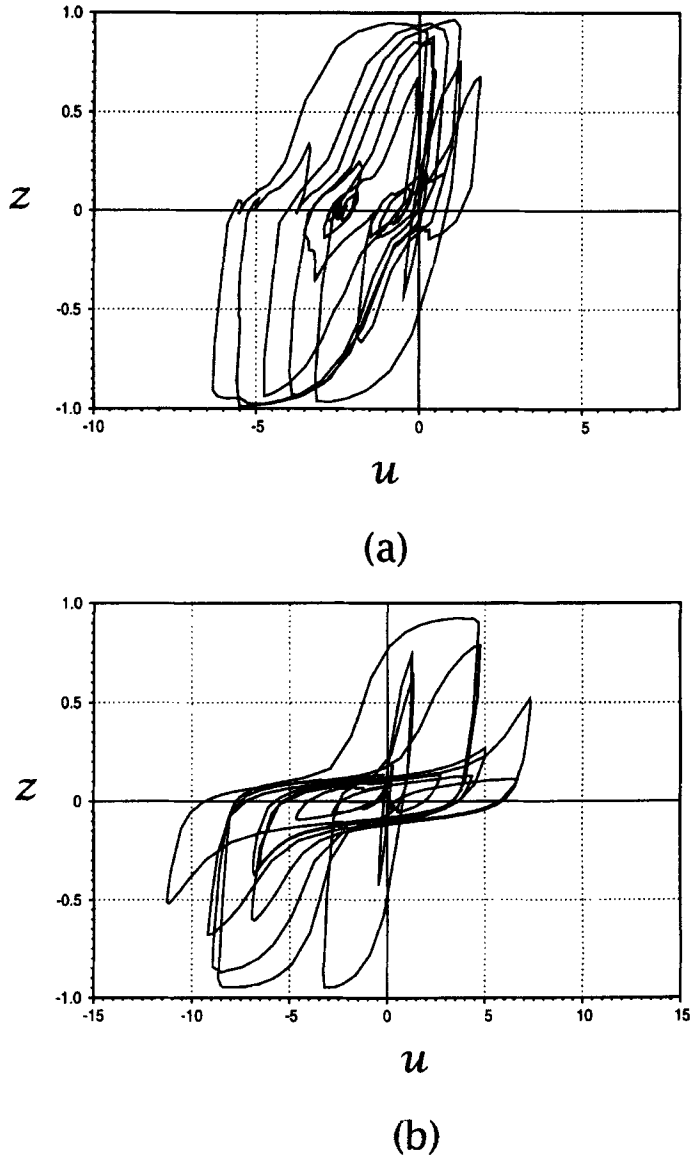

Figure 3. Sample hysteresis plots of a SDOF system under white noise excitation: (a) non-degrading, low pinching ($\zeta_{1_0} = 0{\cdot}85$ and $\delta_\nu = \delta_\eta = 0{\cdot}0$); (b) degrading, high pinching ($\zeta_{1_0} = 0{\cdot}97$, $\delta_\nu = 0{\cdot}005$ and $\delta_\eta = 0{\cdot}05$)

3. STOCHASTIC EQUIVALENT LINEARIZATION

Using state-space formulation with $y_1 = u$, $y_2 = \dot{u}$ and $y_3 = z$, the governing equations (1) and (2), may be rearranged in the form $\dot{\mathbf{y}} = g(\mathbf{y}) + \mathbf{f}$, where

$$\dot{y}_1 = y_2 \tag{3}$$

$$\dot{y}_2 = -\alpha\omega_0^2 y_1 - 2\xi_0\omega_0 y_2 - (1-\alpha)\omega_0^2 y_3 + f(t) \tag{4}$$

$$\dot{y}_3 = \{1{\cdot}0 - \zeta_1 \exp[-(z \operatorname{sgn}(\dot{u}) - qz_u)^2/\zeta_2^2]\} \times \left\{\frac{y_2 - \nu(\beta|y_2||y_3|^{n-1}y_3 - \gamma y_2|y_3|^n)}{\eta}\right\}. \tag{5}$$

Equation (5) may be replaced by the linearized form

$$\dot{y}_3 = C_{e3}y_2 + K_{e3}y_3 \tag{6}$$

where the coefficients C_{e3} and K_{e3} are obtained such that the mean square error $E[e^2]$ is minimized, where

$$e = g_3(\mathbf{y}) - C_{e3}y_2 - K_{e3}y_3 \tag{7}$$

and $g_3(\mathbf{y})$ is the right-hand side of equation (5). Assuming that responses y_2 and y_3 are jointly Gaussian, the linearization coefficients are obtained using a direct linearization scheme[5] as

$$C_{e3} = E\left[\frac{\partial}{\partial y_2}\left\{[1{\cdot}0 - \zeta_1 \exp[-(z \operatorname{sgn}(\dot{u}) - qz_u)^2/\zeta_2^2]] \times \left[\frac{y_2 - \nu(\beta|y_2||y_3|^{n-1}y_3 - \gamma y_2|y_3|^n)}{\eta}\right]\right\}\right] \tag{8}$$

$$K_{e3} = E\left[\frac{\partial}{\partial y_3}\left\{[1{\cdot}0 - \zeta_1 \exp[-(z \operatorname{sgn}(\dot{u}) - qz_u)^2/\zeta_2^2]] \times \left[\frac{y_2 - \nu(\beta|y_2||y_3|^{n-1}y_3 - \gamma y_2|y_3|^n)}{\eta}\right]\right\}\right] \tag{9}$$

where $E[\cdot]$ is the expected value.

Since the degradation and pinching parameters ν, η, ζ_1 and ζ_2 are functions of y_2 and y_3 (see Appendix I), exact evaluation of the expected values is very difficult. Realizing, however, that these parameters are slowly varying, it can be assumed that partial derivatives involving ν, η, ζ_1 and ζ_2 in equations (8) and (9) may be neglected and, by first-order approximation, the parameters may be replaced by μ_ν, μ_η, μ_{ζ_1} and μ_{ζ_2}, respectively.[3] Then, partial differentiation of equations (8) and (9) yields

$$C_{e3} = \frac{1}{\mu_\eta} - \frac{\mu_\nu}{\mu_\eta}(\beta C_1 + \gamma C_2) - \frac{\mu_{\zeta_1}}{\mu_\eta} C_3 + \frac{\mu_{\zeta_1}\mu_\nu}{\mu_\eta}(\beta C_4 + \gamma C_5) \tag{10}$$

and

$$K_{e3} = -\frac{\mu_\nu}{\mu_\eta}(\beta K_1 + \gamma K_2) + 2\frac{\mu_{\zeta_1}}{\mu_\eta \mu_{\zeta_2}^2}(K_3 - qz_u K_4) + \frac{\mu_{\zeta_1}\mu_\nu}{\mu_\eta \mu_{\zeta_2}^2} 2qz_u(\beta K_5 + \gamma K_6) - 2\frac{\mu_{\zeta_1}\mu_\nu}{\mu_\eta \mu_{\zeta_2}^2}(\beta K_7 + \gamma K_8) + n\frac{\mu_{\zeta_1}\mu_\nu}{\mu_\eta}(\beta K_9 + \gamma K_{10}) \tag{11}$$

where the C_i's and the K_i's are given in Appendix II.

The governing equations (3), (4) and (6) are now a set of first-order linear differential equations. They may be rewritten in matrix form as

$$\dot{\mathbf{y}} = \mathbf{G}\mathbf{y} + \mathbf{f} \tag{12}$$

When equation (12) is post-multiplied by $\mathbf{y}^T$, the expectation operators are applied and the resulting equation is added unto its transpose, the covariance equation

$$\dot{\mathbf{S}} = \mathbf{G}\mathbf{S} + \mathbf{S}\mathbf{G}^T + \mathbf{B} \tag{13}$$

for the zero mean time lag covariance matrix $\mathbf{S} = E[\mathbf{y}\mathbf{y}^T]$ is derived.

In equation (13), $\mathbf{B}$ is a matrix of the expected values of the products of the forcing functions and the response vectors,

$$\mathbf{B} = E[\mathbf{f}\mathbf{y}^T + \mathbf{y}\mathbf{f}^T] \tag{14}$$

For simplicity, $f(t)$ is taken in the present work as zero mean Gaussian white noise with constant power spectral density S_0. Filtering and temporal modulation can be easily incorporated into the model. $\mathbf{B}$ has only one non-zero term and can be written as

$$B_{ij} = \delta_{i2}\delta_{2j}\, 2\pi S_0 \tag{15}$$

where δ_{ij} is the Kronecker delta.

The desired response statistics are elements of the zero mean time lag covariance matrix $\mathbf{S}$ obtained by numerical integration of equation (13). The pinching function $h(z)$ and degradation parameters $\nu(\varepsilon)$ and $\eta(\varepsilon)$ are updated at each time step by replacing ε in the approximate equations by its expected value μ_ε. This is obtained by integrating

$$\dot{\mu}_\varepsilon = (1 - \alpha)\omega_0^2 S_{23} \tag{16}$$

parallel with equation (13) to allow updating the deterioration and pinching parameters, and to complete the evaluation of the $\mathbf{G}$ matrix. Numerical integration of equations (13) and (16) yields the non-stationary solution.

4. NUMERICAL STUDIES

This section focuses on verifying the applicability of the linearization solution to the modified BWBN oscillator for a range of cases. Linearization solutions to the parent forms of the modified BWBN model have been studied and verified by simulation.[2,3,41,43] Graphical comparisons are made since theoretical bounds on the errors of response statistics obtained by approximate methods have not yet been completely established in structural dynamics applications.[27] Simulation results are obtained from 200 response samples.

4.1. Base system

Consider a SDOF base system with the following properties: $\omega_0 = 4{\cdot}7$ rad/s, $\xi_0 = 0{\cdot}10$, $\alpha = 0{\cdot}10$, $\beta = 1{\cdot}5$, $\gamma = -0{\cdot}5$, $n = 1$, $q = 0{\cdot}10$, $\zeta_{1_0} = 0{\cdot}96$, $\lambda = 0{\cdot}10$, $p = 1$, $\psi_0 = 0{\cdot}20$, $\delta_\psi = 0{\cdot}01$, $\delta_\nu = 0{\cdot}005$ and $\delta_\eta = 0{\cdot}05$. Three levels of white noise excitation ($S_0 = 0{\cdot}1$, $0{\cdot}5$ and $1{\cdot}0$, corresponding to an average peak acceleration—based on 500 realizations—of $0{\cdot}31g$, $0{\cdot}68g$ and $0{\cdot}96g$, respectively, where g is the acceleration of gravity) are used to obtain the zero time lag covariance matrix response, starting with zero initial conditions. Figures 4(a)–4(d) show comparisons of simulation and linearization results. It is seen that linearization results for this system generally agree with simulation. The root mean square (RMS) displacement σ_u, RMS velocity $\sigma_{\dot{u}}$, RMS restoring force σ_z and mean dissipated energy μ_ε are estimated very closely at all excitation levels.

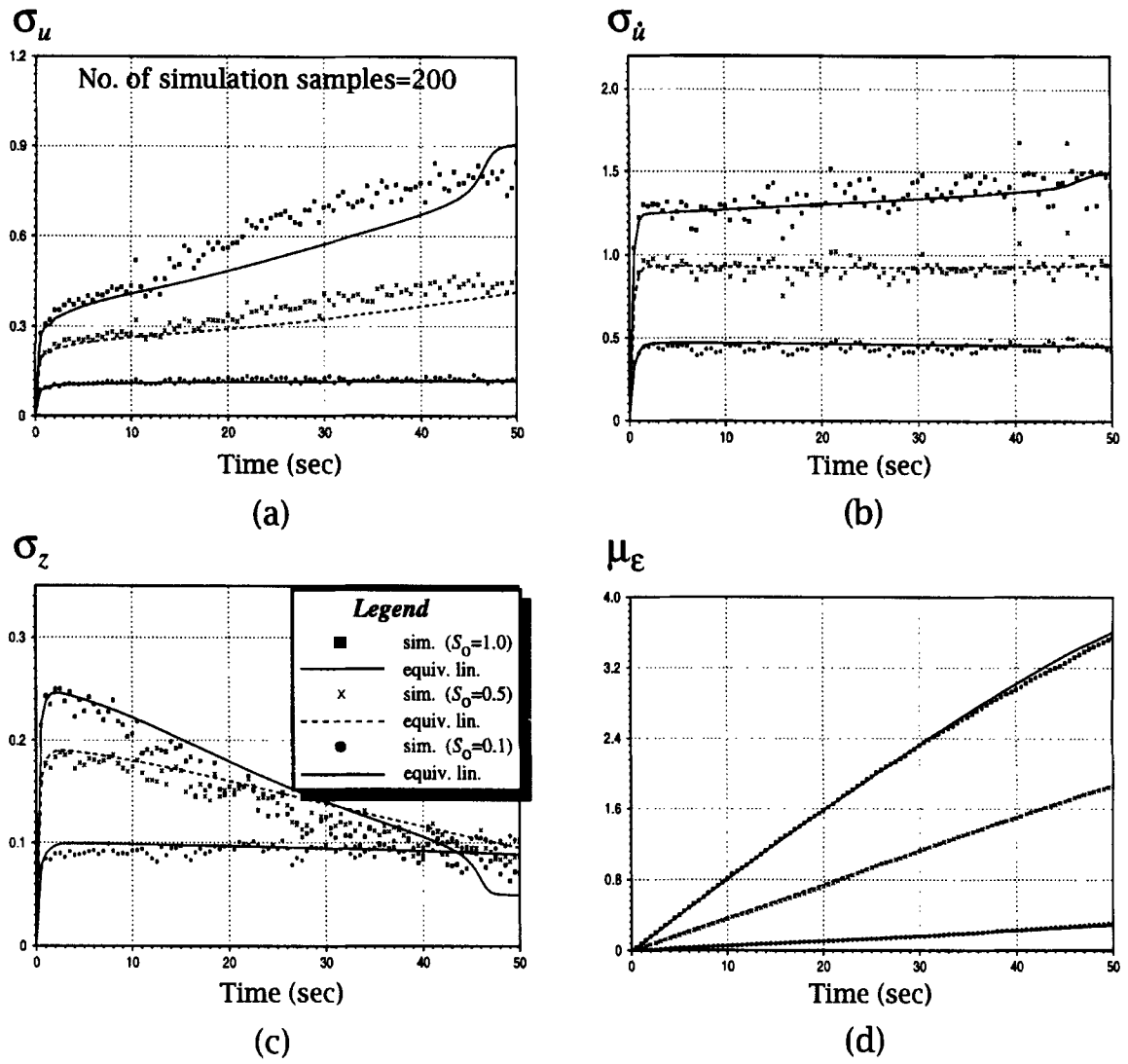

Figure 4. Non-stationary response of a SDOF system under stationary white noise input (base system): (a) root mean square (RMS) displacement; (b) RMS velocity; (c) RMS restoring force; and (d) mean energy dissipation

The effects of changing model parameter values on the accuracy of response statistics obtained by linearization are considered next. The parameters of the base system are changed one at a time. For example, to evaluate the effect of system frequency on the accuracy of linearization results, all the parameters of the base system, except for the frequency, are fixed. The frequency values given in Table I are used for analysis and the linearization and simulation results for each frequency level are compared. The process is repeated for all the parameters listed in Table I. Thus, for all systems studied, the base properties given in this section are used unless otherwise stated. Response statistics are obtained only for white noise excitation level $S_0 = 0{\cdot}5$.

4.2. Effect of system properties and model shape parameters

The effects of varying system properties (frequency, ω_0, and damping ratio, ξ_0), hysteresis shape parameters (α and n), and degradation parameters (δ_ν and δ_η) on the accuracy of response statistics obtained by

Table I. Parameter values considered in numerical studies

Parameter	Range of values min		max
System properties & hysteresis parameters			
ω_0 (rad/s)	0·80	2·00	6·50
ξ_0	0·01		0·20
α	0·05		0·50
n	1·00		12·00
Degradation parameters			
δ_ν	0·00		0·20
δ_η	0·00		0·20
Pinching parameters			
ζ_{10}	0·70		0·98
q	0·00		0·20
p	1·00		2·00
ψ_0	0·01		0·50
δ_ψ	0·00		0·20
λ	0·01		0·60

equivalent linearization are studied. Shape parameter values for β and γ are fixed at 1·5 and $-0·5$, respectively (case where $\beta + \gamma > 0$ and $\gamma - \beta \leqslant 0$). First, three frequency levels are considered (see Table I). Figures 5(a)–5(d) show comparisons of simulation and linearization results. The linearized σ_u and $\sigma_{\dot{u}}$ responses agree very well with simulation results. Figure 5(c) shows that the σ_z is estimated very well when $\omega_0 = 6·5$ rad/s, but are slightly overestimated when $\omega_0 = 2·0$ rad/s and underestimated when $\omega_0 = 0·8$ rad/s. Mean energy dissipation is reasonably estimated at all frequency levels [Figure 5(d)].

The accuracy of RMS restoring force σ_z obtained by equivalent linearization is significantly influenced by system frequency, especially at low-frequency levels. This could be significant since some structural systems tend to loosen at the joints after heavy shaking, resulting in a decreased system frequency (or longer natural period). Thus, in studying the influence of other model parameters on the accuracy of response statistics obtained by linearization, two frequency levels are considered (the base system frequency, $\omega_0 = 4·7$ rad/s, and a low-frequency system, $\omega_0 = 0·8$ rad/s). For brevity, response comparisons presented from hereon are limited to RMS displacement σ_u only.

The effect of damping ratio ξ_0 on the accuracy of response statistics obtained by equivalent linearization is demonstrated in Figure 6(a). σ_u's are estimated extremely well at both levels of ξ_0, when $\omega_0 = 0·8$ rad/s, but are underestimated slightly when $\xi_0 = 0·01$ and $\omega_0 = 4·7$ rad/s.

With two levels of rigidity ratio ($\alpha = 0·05$ and $\alpha = 0·50$), linearization results agree very closely with simulation results except when $\alpha = 0·05$ and $\omega_0 = 4·7$ rad/s, where σ_u is underestimated from $t \geqslant 15$ s [Figure 6(b), right].

Two levels of n ($n = 1$ and $n = 12$; the latter case corresponds to a nearly elastoplastic case in the z–u plane) are considered. Figure 6(c) shows that linearization results compare generally well with those from simulation. σ_u is only slightly underestimated when $n = 1$, $\omega_0 = 4·7$ rad/s, at $t \geqslant 20$ s. Note that increasing the value of n (i.e. $n > 1$) not only improves the accuracy of the linearization solution for this system but effectively reduces the Bouc–Wen model's violation of the Drucker's postulate of plasticity,[26] in general.

Two cases of strength and stiffness degradations were analysed: (1) no degradation ($\delta_\nu = 0$; $\delta_\eta = 0$), and (2) severe degradation ($\delta_\nu = 0·2$; $\delta_\eta = 0·2$). The plots are not shown here but σ_u estimates from linearization compare satisfactorily with those from simulation.

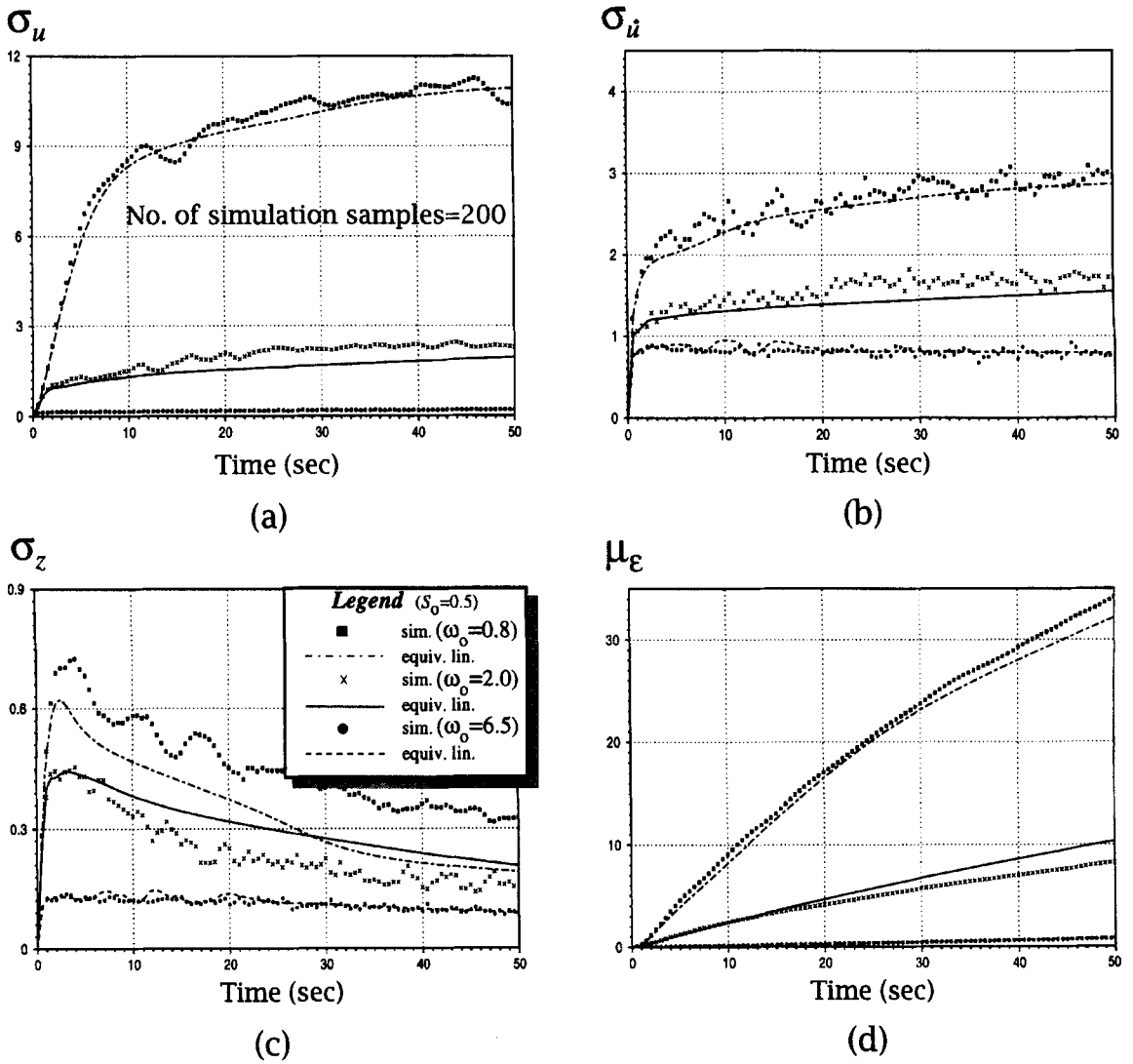

Figure 5. Non-stationary response of a SDOF system under stationary white noise input (effect of system frequency ω_0): (a) RMS displacement; (b) RMS velocity; (c) RMS restoring force; and (d) mean energy dissipation

4.3. Effect of pinching parameters

The effect of varying pinching parameters ζ_{10}, q, p, ψ_0, δ_ψ and λ on the accuracy of response statistics obtained by equivalent linearization are studied next. First, a low pinching system ($\zeta_{10} = 0{\cdot}7$) is compared with a high pinching system ($\zeta_{10} = 0{\cdot}98$). Figure 7(a) shows that the linearization solutions are reasonably good in all cases.

With two pinching levels ($q = 0$ and $q = 0{\cdot}2$; recall that, the original BWBN model is obtained when $q = 0$), Figure 7(b) shows that linearization results estimate σ_u sufficiently well.

The influence of p ($p = 1{\cdot}0$ and $p = 2{\cdot}0$), a constant that controls the rate of initial drop in slope, on the accuracy of response statistics obtained by equivalent linearization is shown in Figure 7(c). Linearization solutions of σ_u compare favourably with those obtained by simulation for both levels of p and both levels of system frequency. Note that when $\omega_0 = 0{\cdot}8$ rad/s, the change of p from 1·0 to 2·0 does not affect the response statistics obtained by either the linearization technique or the simulation method.

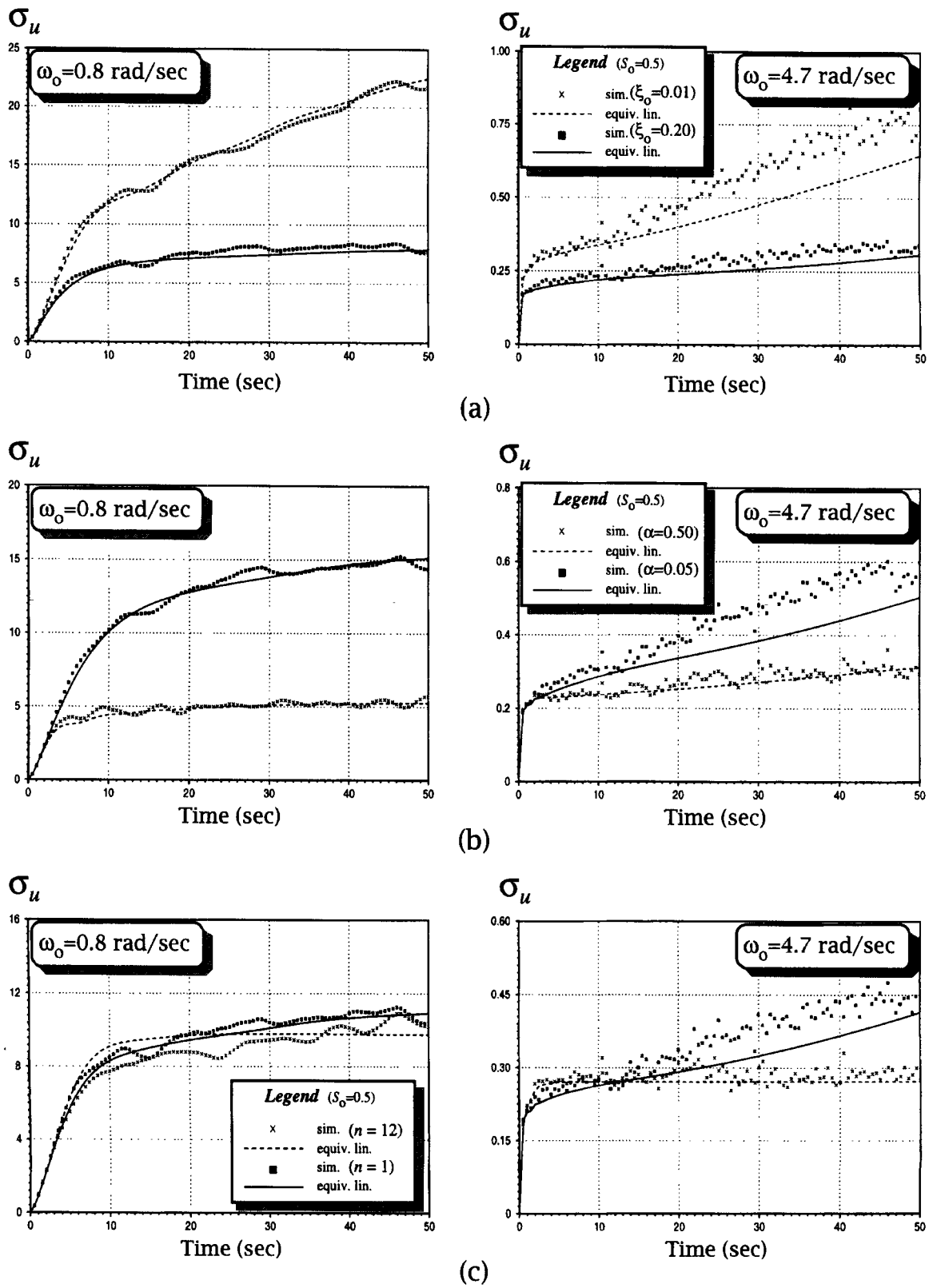

Figure 6. Non-stationary RMS displacement response of a SDOF system under stationary white noise input (effect of system properties and hysteresis shape parameters): (a) damping ratio ζ_0; (b) α; and (c) n

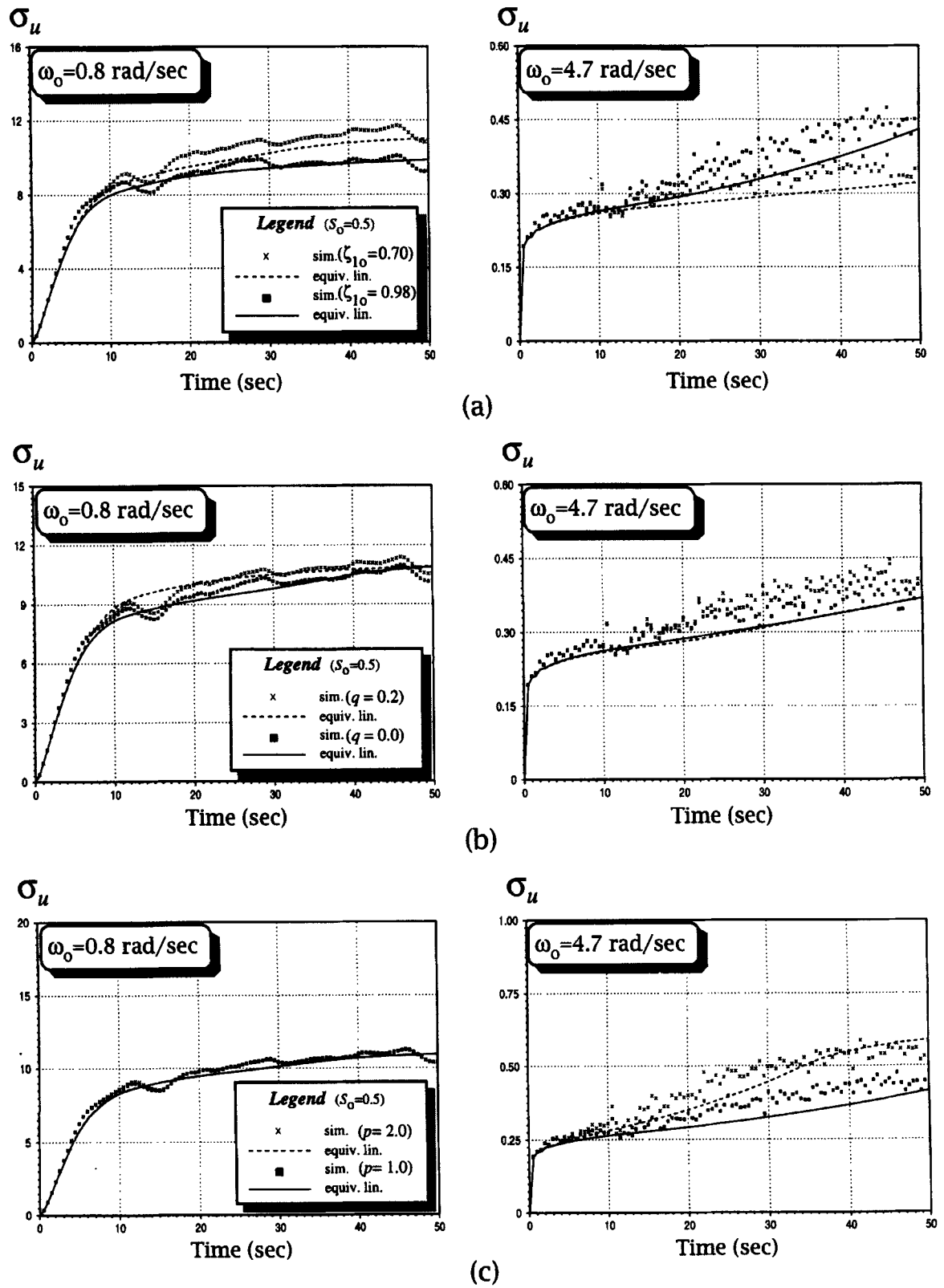

Figure 7. Non-stationary RMS displacement response of a SDOF system under stationary white noise input (effect of pinching parameters): (a) ξ_{10}, (b) q, and (c) p

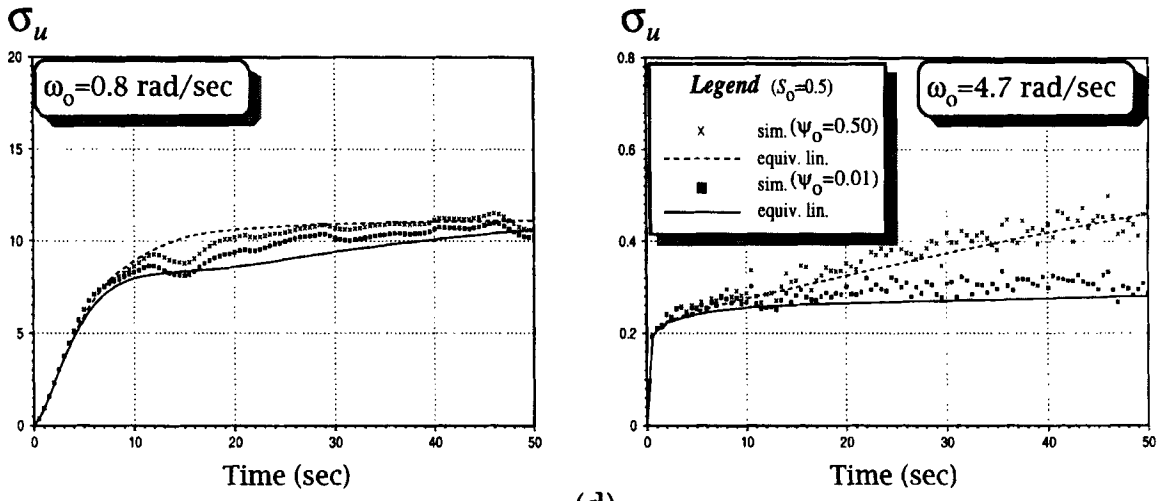

(d)

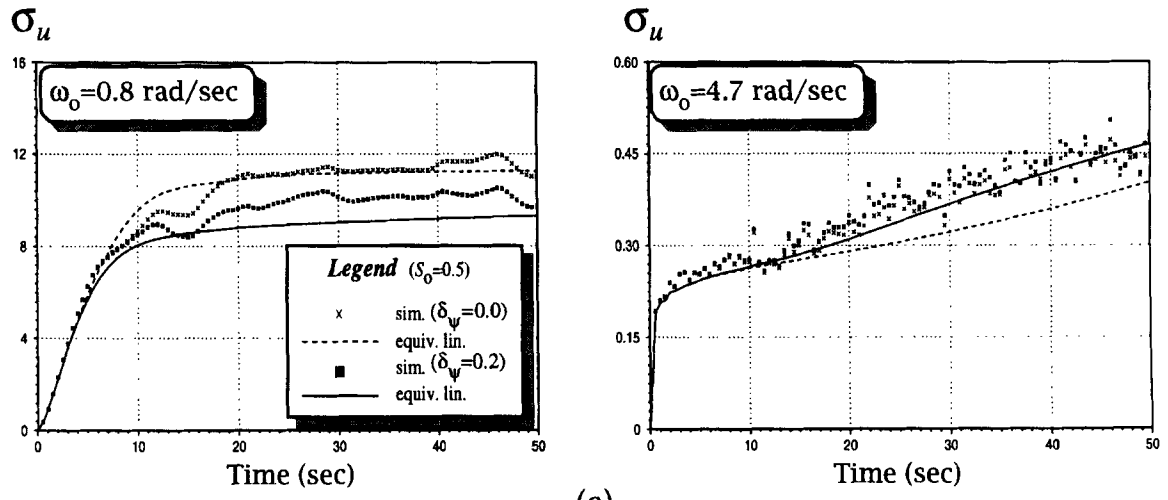

(e)

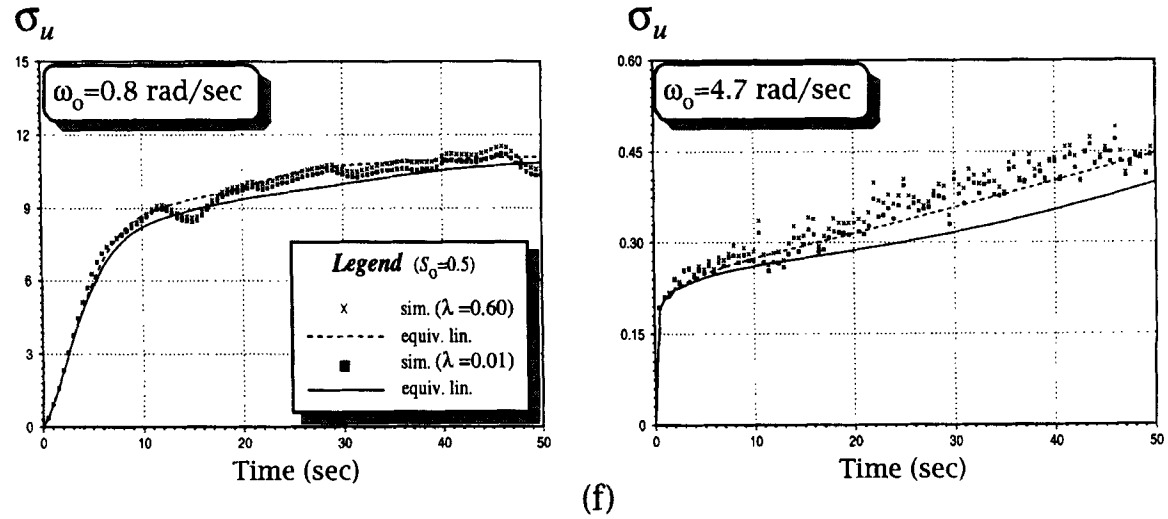

(f)

Figure 7. (d) ψ_0, (e) δ_ψ, and (f) λ

Two levels of ψ_0 ($\psi_0 = 0{\cdot}01$ and $\psi_0 = 0{\cdot}50$), a parameter that contributes to the amount of pinching, are considered. Linearization solutions compare very well with those by simulation [Figure 7(d)].

The influence of δ_ψ ($\delta_\psi = 0$ and $\delta_\psi = 0{\cdot}2$) is studied. Figure 7(e) shows that linearization estimates of σ_u are slightly lower than those of simulation when $\omega_0 = 0{\cdot}8$ rad/s, $\delta_\psi = 0{\cdot}2$ and $t \geqslant 18$ s and when $\omega_0 = 4{\cdot}7$ rad/s, $\delta_\psi = 0$ and $t \geqslant 18$ s.

Finally, linearization and simulation results are compared when $\lambda = 0{\cdot}01$ and $\lambda = 0{\cdot}60$. Figure 7(f) shows that this parameter has a minor influence on σ_u. Linearization results underestimate σ_u slightly when $\omega_0 = 4{\cdot}7$ rad/s, but are generally good, otherwise.

4.4. Comments

Considering the range of cases (summarized in Table I) studied herein, it can be generally stated that equivalent linearization gives reasonably good estimates of response statistics. Results of numerical studies have shown that, for structures with low system natural frequency (e.g. $\omega_0 = 0{\cdot}8$ rad/s), pinching parameters p and λ do not significantly affect mean-square response statistics, and may, thus, be set to some reasonable constant. It was also observed that the accuracy of σ_z linearization estimates (not shown here; see Reference 52) was not as good as that of σ_u estimates (Figures 6 and 7), for a few systems with low-frequency (e.g. $\omega_0 = 0{\cdot}8$ rad/s) and under high excitation level (e.g. $S_0 = 0{\cdot}5$ and $1{\cdot}0$, when the original non-linear system responses deviate significantly from a Gaussian law).

Although the comparisons of simulation and linearization results showed generally good agreement, it is wise to conduct prior verification of a representative set of response statistics derived by equivalent linearization by comparing them with Monte Carlo simulations. Only then should the method be used repeatedly as the basis of critical technical estimations regarding a particular problem of interest.[27]

5. SUMMARY AND CONCLUSIONS

A modification of the Bouc–Wen–Baber–Noori hysteretic restoring force model, that allows general off-the-origin pinching, was used in stochastic equivalent linearization of SDOF structural systems. The severity and rate of pinching are controlled by the hysteretic energy dissipation and the pinching level can be specified to match experimental data. The new model can produce a wide variety of hysteresis shapes, degradations, and pinching behaviour to model a whole gamut of possible combinations of engineering materials and structural configurations as long as appropriate structural models for random vibration analysis can be constructed, and hysteresis parameters are known. It has potential applications in random vibration studies of laterally loaded piles, and reinforced concrete [e.g. Figures 1(a) and 1(b)], steel [Figures 1(c) and 1(d)], reinforced gypsum [Figure 1(e)] and timber [Figure 1(f)] structural systems. For practical purposes, system identification techniques should be used to identify the hysteresis model parameters for these systems from test data.

The non-stationary response statistics of SDOF systems under stochastic excitations were obtained by Monte Carlo simulation and equivalent linearization. The equivalent linearization coefficients presented herein can be used directly in random vibration studies of MDOF systems, using shear beam (e.g. References 3 and 8) or discrete hinge structural models (e.g. References 9–12). It was shown in this paper that, for a range of practical cases, the use of equivalent linearization technique is sufficiently accurate in obtaining relevant response statistics and that it can be used in lieu of simulation. There may be a few cases, however, where the mean-square responses may be severely underestimated. Although an error-correction scheme[31] can be used to improve response estimates, a verification study should be performed before the method is used repeatedly as the basis of critical technical estimations regarding a particular engineering problem. Results can also help identify an optimum model that can be used for further analysis. Numerical studies in the present work, for example, showed that for low-frequency structural systems, some hysteresis parameters may be set to a constant value *a priori* to reduce the number of model parameters that needs to be estimated or identified, and to simplify further random vibration analysis and/or performance evaluation studies.

APPENDIX I

Degradation and pinching functions

Strength and stiffness degradations are modelled, respectively, by[3]

$$\nu(\varepsilon) = 1{\cdot}0 + \delta_\nu \varepsilon \tag{17}$$

$$\eta(\varepsilon) = 1{\cdot}0 + \delta_\eta \varepsilon$$

where ε is the hysteretic energy dissipation, given by

$$\varepsilon = (1 - \alpha)\omega_0^2 \int_{t_0}^{t_f} z\dot{u}\, \mathrm{d}t\,. \tag{18}$$

Energy dissipation is a good measure of cumulative damage under stress reversals because it mirrors the loading history and parallels the process of damage evolution.[21,23]

Pinching should be induced during loading only; that is, when $z\dot{u}$ or $\mathrm{sgn}(z)\cdot\mathrm{sgn}(\dot{u})$ is positive, where $\mathrm{sgn}(\cdot)$ is the signum function. This is achieved by setting $h(z)$ as[24]

$$h(z) = 1{\cdot}0 - \zeta_1 \exp\left[-(z\,\mathrm{sgn}\,(\dot{u}) - qz_u)^2/\zeta_2^2\right] \tag{19}$$

where $0 \leqslant \zeta_1 < 1$ controls the severity of pinching or magnitude of initial drop in slope $(\mathrm{d}z/\mathrm{d}u)$, ζ_2 causes the pinching region to spread, z_u is the ultimate value of z given by

$$z_u = \left[\frac{1}{\nu(\beta + \gamma)}\right]^{1/n} \tag{20}$$

and q is a constant that sets a fraction of z_u as the pinching level. Equation (19) is an extended and improved form of the pinching function originally proposed in Reference 43. If $q = 0$, the Baber and Noori[43] pinching function is obtained. Both ζ_1 and ζ_2 vary non-linearly with the total energy dissipated by the hysteretic element, ε, and are given as

$$\zeta_1(\varepsilon) = \zeta_{1_0}[1{\cdot}0 - \exp(-p\varepsilon)] \tag{21}$$

$$\zeta_2(\varepsilon) = (\psi_0 + \delta_\psi \varepsilon)(\lambda + \zeta_1)$$

where p is the constant that controls the rate of initial drop in slope, ζ_{1_0} is the measure of total slip; ψ_0 is the parameter that contributes to the amount of pinching, δ_ψ is the constant specified for the desired rate of pinching spread, and λ is the small parameter that controls the rate of change of ζ_2 as ζ_1 changes. More details about $h(z)$ and its parameters are given in References 24, 43 and 52.

APPENDIX II

Elements of the linearization coefficients

Derivation details of the elements of the linearization coefficients in equations (10) and (11) are given in Reference 52. In the following, σ_2 and σ_3 are the respective root mean square values of y_2 and y_3, and ρ_{23} is their correlation coefficient:

$$C_1 = \frac{1}{\pi}(2)^{n/2}\,\sigma_3^n\,\Gamma\left(\frac{n+2}{2}\right) I_{sn} \tag{22}$$

$$C_2 = \frac{1}{\sqrt{\pi}}(2)^{n/2}\,\sigma_3^n\,\Gamma\left(\frac{n+1}{2}\right) \tag{23}$$

$$C_3 = \frac{\mu_{\zeta_2}}{\sqrt{2\sigma_3^2 + \mu_{\zeta_2}^2}} e^{-\Delta_1} \operatorname{erfc}\left(\frac{-\Delta_3}{\sqrt{2}}\right) \tag{24}$$

$$C_4 = \frac{1}{\sqrt{2\pi}\sigma_3} e^{-\Delta_1} [I_{GL}(1, n) - I_{GL}(-1, n)] \tag{25}$$

$$C_5 = \frac{1}{\sqrt{2\pi}\sigma_3} e^{-\Delta_1} [I_{GL}(1, n) + I_{GL}(-1, n)] \tag{26}$$

$$K_1 = \frac{n}{\pi} (2)^{n/2} \sigma_2 \sigma_3^{n-1} \Gamma\left(\frac{n+2}{2}\right)\left[\frac{2}{n}(1 - \rho_{23}^2)^{(n+1)/2} + \rho_{23} I_{sn}\right] \tag{27}$$

$$K_2 = \frac{n}{\sqrt{\pi}} (2)^{n/2} \rho_{23} \sigma_2 \sigma_3^{n-1} \Gamma\left(\frac{n+1}{2}\right) \tag{28}$$

$$K_3 = \frac{\mu_{\zeta_2}}{\sqrt{2\sigma_3^2 + \mu_{\zeta_2}^2}} \frac{\sigma_2}{\sigma_3} e^{-\Delta_1} \times\left[\rho_{23}(\mu_{1c}^2 + \sigma_{1c}^2) \operatorname{erfc}\left(\frac{-\Delta_3}{\sqrt{2}}\right) + \sqrt{\frac{2}{\pi}} \mu_{1c} \Delta_2 e^{-\Delta_3^2/2}\right] \tag{29}$$

$$K_4 = \frac{\mu_{\zeta_2}}{\sqrt{2\sigma_3^2 + \mu_{\zeta_2}^2}} \frac{\sigma_2}{\sigma_3} e^{-\Delta_1} \times\left[\rho_{23}\mu_{1c} \operatorname{erfc}\left(\frac{-\Delta_3}{\sqrt{2}}\right) + \sqrt{\frac{2}{\pi}} \Delta_2 e^{-\Delta_3^2/2}\right] \tag{30}$$

$$K_5 = \frac{1}{\pi}\frac{\sigma_2}{\sigma_3} e^{-\Delta_1} \left\{\sqrt{1 - \rho_{23}^2}\, [I_{sum}(1, n) - I_{sum}(-1, n)] + \sqrt{\frac{\pi}{2}}\frac{\rho_{23}}{\sigma_3} [I_{GL}(1, n+1) + I_{GL}(-1, n+1)]\right\} \tag{31}$$

$$K_6 = \frac{1}{\pi}\frac{\sigma_2}{\sigma_3} e^{-\Delta_1} \left\{\sqrt{1 - \rho_{23}^2}\, [I_{sum}(1, n) + I_{sum}(-1, n)] + \sqrt{\frac{\pi}{2}}\frac{\rho_{23}}{\sigma_3} [I_{GL}(1, n+1) - I_{GL}(-1, n+1)]\right\} \tag{32}$$

$$K_7 = \frac{1}{\pi}\frac{\sigma_2}{\sigma_3} e^{-\Delta_1} \left\{\sqrt{1 - \rho_{23}^2}\, [I_{sum}(1, n+1) + I_{sum}(-1, n+1)] + \sqrt{\frac{\pi}{2}}\frac{\rho_{23}}{\sigma_3} [I_{GL}(1, n+2) - I_{GL}(-1, n+2)]\right\} \tag{33}$$

$$K_8 = \frac{1}{\pi}\frac{\sigma_2}{\sigma_3} e^{-\Delta_1} \left\{\sqrt{1 - \rho_{23}^2}\, [I_{sum}(1, n+1) - I_{sum}(-1, n+1)] + \sqrt{\frac{\pi}{2}}\frac{\rho_{23}}{\sigma_3} [I_{GL}(1, n+2) + I_{GL}(-1, n+2)]\right\} \tag{34}$$

$$K_9 = \frac{1}{\pi}\frac{\sigma_2}{\sigma_3}\mathrm{e}^{-\Delta_1}\left\{\sqrt{1-\rho_{23}^2}\,[I_{\mathrm{sum}}(1,n-1)+I_{\mathrm{sum}}(-1,n-1)]\right.$$
$$\left.+\sqrt{\frac{\pi}{2}}\frac{\rho_{23}}{\sigma_3}\,[I_{\mathrm{GL}}(1,n)-I_{\mathrm{GL}}(-1,n)]\right\} \tag{35}$$

$$K_{10} = \frac{1}{\pi}\frac{\sigma_2}{\sigma_3}\mathrm{e}^{-\Delta_1}\left\{\sqrt{1-\rho_{23}^2}\,[I_{\mathrm{sum}}(1,n-1)-I_{\mathrm{sum}}(-1,n-1)]\right.$$
$$\left.+\sqrt{\frac{\pi}{2}}\frac{\rho_{23}}{\sigma_3}\,[I_{\mathrm{GL}}(1,n)+I_{\mathrm{GL}}(-1,n)]\right\} \tag{36}$$

where I_{sn} is given by

$$I_{\mathrm{sn}} = 2\,\mathrm{sgn}\,(\rho_{23})\int_{\theta_0}^{\pi/2}\sin^n\theta\,\mathrm{d}\theta$$
$$\theta_0 = \tan^{-1}\left(\frac{\sqrt{1-\rho_{23}^2}}{\rho_{23}}\right) \tag{37}$$

I_{GL} is a Gauss–Laguerre quadrature:

$$I_{\mathrm{GL}}(f_i,m) = \int_0^\infty \exp\left[-\frac{1}{2}\left(\frac{y_3 - f_i\mu_{1c}}{\sigma_{1c}}\right)^2 + y_3\right]$$
$$\times\left[1+f_i\,\mathrm{erf}\left(\frac{\rho_{23}y_3}{\sqrt{2}\sigma_3\sqrt{1-\rho_{23}^2}}\right)\right]y_3^m\,\mathrm{e}^{-y_3}\,\mathrm{d}y_3 \tag{38}$$

I_{sum} is a standard summation:

$$I_{\mathrm{sum}}(f_i,m) = \sigma_{2c}\mathrm{e}^{-\Delta_3^2/2}\sum_{k=0}^{m}\binom{m}{k}(\mu_{2c})^{m-k}\sigma_{2c}^k(2)^{(k-1)/2}$$
$$\times f_{\mathrm{sgn}}\left[\gamma\left(\frac{k+1}{2},\frac{\mu_{2c}^2}{2\sigma_{2c}^2}\right)-\Gamma\left(\frac{k+1}{2}\right)\right] \tag{39}$$

$$f_{\mathrm{sgn}} = \begin{cases}(-1)^k & \text{if } f_i = 1\\ (-1)^{m-k-1} & \text{if } f_i = -1\end{cases}$$

the constants are

$$\Delta_1 = \frac{q^2 z_u^2}{2\sigma_3^2+\mu_{\zeta_2}^2} \tag{40}$$

$$\Delta_2 = \sqrt{\sigma_3^2(1-\rho_{23}^2)+\rho_{23}^2\sigma_{1c}^2} \tag{41}$$

$$\Delta_3 = \frac{\rho_{23}\mu_{1c}}{\Delta_2} \tag{42}$$

$$\mu_{1c} = \frac{2qz_u\sigma_3^2}{2\sigma_3^2+\mu_{\zeta_2}^2} \tag{43}$$

$$\sigma_{1c} = \frac{\mu_{\zeta_2}\sigma_3}{\sqrt{2\sigma_3^2 + \mu_{\zeta_2}^2}} \tag{44}$$

$$\mu_{2c} = \frac{\mu_{1c}\sigma_3^2(1 - \rho_{23}^2)}{\Delta_2^2} \tag{45}$$

$$\sigma_{2c} = \frac{\sigma_{1c}\sigma_3\sqrt{1 - \rho_{23}^2}}{\Delta_2} \tag{46}$$

$\mathrm{erf}(\cdot)$ is the error function, $\mathrm{erfc}(\cdot)$ is the complementary error function, $\Gamma(\cdot)$ is the gamma function and $\gamma(a, b)$ is the incomplete gamma function.

REFERENCES

1. Y.-K. Wen, 'Method for random vibration of hysteretic systems', *J. eng. mech. div. ASCE* **102**, 249–263 (1976).
2. Y.-K. Wen, 'Equivalent linearization for hysteretic systems under random excitation', *J. appl. mech. ASME* **47**, 150–154 (1980).
3. T. T. Baber and Y.-K. Wen, 'Random vibration of hysteretic degrading systems', *J. eng. mech. ASCE* **107**, 1069–1089 (1981).
4. R. Bouc, 'Forced vibration of mechanical systems with hysteresis', Abstract. *Proc. 4th conf. on nonlinear oscillation*, Prague, Czechoslovakia, 1967.
5. T. S. Atalik and S. Utku, 'Stochastic linearization of multidegree of freedom nonlinear systems', *Earthquake eng. struct. dyn.* **4**, 411–420 (1976).
6. Y.-K. Wen, 'Stochastic response and damage analysis of inelastic structures', *Probab. eng. mech.* **1**(1), 49–57 (1986).
7. Y.-K. Wen, 'Methods of random vibration for inelastic structures', *Appl. mech. rev. ASME* **42**(2), 39–52 (1989).
8. T.-P. Chang, T. Mochio and E. Samaras, 'Seismic response analysis of nonlinear structures', *Probab. eng. mech.* **1**, 157–166 (1986).
9. T. T. Baber and Y.-K. Wen, 'Stochastic response of multistorey yielding frames', *Earthquake eng. struct. dyn.* **10**, 403–416 (1982).
10. T. T. Baber, 'Nonzero mean random vibration of hysteretic systems', *J. eng. mech.ASCE* **110**, 1036–1049 (1984).
11. T. T. Baber, 'Modal analysis for random vibration of hysteretic frames', *Earthquake eng. struct. dyn.* **14**, 841–859 (1986).
12. T. T. Baber, 'Nonzero mean random vibration of hysteretic frames', *Comput. struct.***23**, 265–277 (1986).
13. Y. J. Park, Y.-K. Wen and A. H.-S. Ang, 'Random vibration of hysteretic systems under bi-directional ground motions', *Earthquake eng. struct. dyn.* **14**, 543–557 (1986).
14. Y.-K. Wen and C. H. Yeh, 'Biaxial and torsional response of inelastic structures under random excitation', *Struct. safety* **6**, 137–152 (1989).
15. F. Casciati and L. Faravelli, 'Stochastic equivalent linearization for 3-D frames', *J. eng. mech. ASCE* **114**, 1760–1771 (1988).
16. F. Casciati, 'Stochastic dynamics of hysteretic media', *Struct. safety* **6**, 259–269 (1989).
17. I. Simulescu, T. Mochio and M. Shinozuka, 'Equivalent linearization method in nonlinear FEM', *J. eng. mech. ASCE* **115**, 475–492 (1989).
18. J. E. A. Pires, Y.-K. Wen and A. H.-S. Ang, 'Stochastic analysis of liquefaction under earthquake loading', in Civil Eng. Studies, structural Research Series No. 504, Univ. of Illinois at Urbana-Champaign, Urbana, IL, 1983.
19. M. C. Constantinou and I. G. Tadjbakhsh, 'Hysteretic dampers in base isolation: random approach', *J. struct. eng. ASCE* **111**, 705–721 (1985).
20. R. H. Sues, Y.-K. Wen and A. H.-S. Ang, 'Stochastic evaluation of seismic structural performance', *J. struct. eng. ASCE* **111**, 1204–1218 (1985).
21. Y. J. Park, A. H.-S. Ang and Y.-K. Wen, 'Seismic damage analysis of reinforced concrete buildings', *J. struct. eng. ASCE* **111**, 740–757 (1985).
22. D. F. Eliopoulos and Y.-K. Wen, 'Evaluation of response statistics of moment resisting steel frames under seismic excitation', in P. D. Spanos and C. A. Brebbia (eds) *Computational Stochastic Mechanics*, Computational Mechanics Publications, Boston and Elsevier Applied Science, New York, 1991, pp. 673–684.
23. Y. H. Kwok, 'Seismic damage analysis and design of unreinforced masonry buildings', *Ph.D. Thesis*, Univ. of Illinois at Urbana-Champaign, Urbana, IL, 1987.
24. G. C. Foliente. 'Hysteresis modeling of wood joints and structural systems', *J. struct. eng. ASCE* **121**, 1013–1022 (1995).
25. C. W. Wong, Y. Q. Ni and S. L. Lau, 'Steady-state oscillation of hysteretic differential model. I: response analysis', *J. eng. mech. ASCE* **120**, 2271–2298 (1994).
26. C. W. Wong, Y. Q. Ni and J. M. Ko, 'Steady-state oscillation of hysteretic differential model. II: performance analysis', *J. eng. mech. ASCE* **120**, 2299–2325 (1994).
27. J. B. Roberts and P. D. Spanos, *Random Vibration and Statistical Linearization*, Wiley, West Sussex, England, 1990.
28. R. L. Grossmayer and W. D. Iwan, 'A linearization scheme for hysteretic systems subjected to random excitations', *Earthquake eng. struct. dyn.* **9**, 171–185 (1981).
29. I. Elishakoff, 'Method of stochastic linearization revised and improved', in P. D. Spanos and C. A. Brebbia (eds), *Computational Stochastic Mechanics*, Computational Mechanics Publication, Boston and Elsevier Applied Science, New York, 1991, pp. 101–111.
30. H. J. Pradlwarter and G. I. Schuëller, 'Equivalent linearization—a suitable tool for analyzing MDOF-systems', *Probab. eng. mech.* **8**, 115–126 (1992).
31. Y. J. Park, 'Equivalent linearization for seismic response. I: formulation and error analysis', *J. eng. mech. ASCE* **118**, 2207–2226 (1992).

32. B. F. Bergman and L. A. Spencer, 'On the reliability of a simple hysteretic system', *J. eng. mech. ASCE* **111**, 1502–1514 (1985).
33. T. Mochio, 'Stochastic response of nonlinear multi-degrees-of-freedom structures subjected to combined random loads', in P. D. Spanos and C. A. Brebbia (eds), *Computational Stochastic Mechanics*, Computational Mechanics Publications, Boston and Elsevier Applied Science, New York, 1991, pp. 255–265.
34. N. C. Hampl and G. I. Schuëller, 'Probability densities of the response of nonlinear structures under stochastic dynamic excitation', *Probab. eng. mech.* **4**, 2–9 (1989).
35. H. Davoodi and M. N. Noori, 'Extension of an Itô-based general approximation technique for random vibration of a BBW general hysteresis model. Part II: non-Gaussian analysis', *J. sound vib.* **140**, 319–339 (1989).
36. M. Yar and J. K. Hammond, 'Stochastic response of an exponentially hysteretic system though stochastic averaging', *Probab. eng. mech.* **2**, 147–155 (1987).
37. A. Naess and J. M. Johnsen, 'The path integral solution technique applied to the random vibration of hysteretic systems', in P. D. Spanos and C. A. Brebbia (eds), *Computational Stochastic Mechanics*, Computational Mechanics Publications, Boston, and Elsevier Applied Science, New York, 1991, pp. 279–291.
38. G. Cai and Y. K. Lin, 'A new approximate solution technique for random vibration of hysteretic systems', in A. H.-S. Ang, M. Shinozuka, G. I. Schüeller (eds), *Structural Safety and Reliability, Proc. ICOSSAR '89*, Vol. 2, ASCE, New York, 1989, pp. 1209–1216.
39. R. H. Sues, S. T. Mau and Y.-K. Wen, 'System identification of degrading hysteretic restoring forces', *J. eng. mech. ASCE* **114**, 833–846, (1988).
40. F. Casciati, 'Nonlinear stochastic dynamics of large structural systems by equivalent linearization', in N. C. Lind (ed.), *Reliability and Risk Analysis in Civil Engineering* 2, University of Waterloo, Canada, 1987, pp. 1165–1172.
41. M. N. Noori, 'Random vibration of degrading systems with general hysteretic behavior', *Ph.D. Thesis*, Univ. of Virginia, Charlottesville, VA, 1984.
42. T. T. Baber and M. N. Noori, 'Random vibration of degrading, pinching systems', *J. eng. mech. ASCE* **111**, 1010–1026 (1985).
43. T. T. Baber and M. N. Noori, 'Modeling general hysteresis behavior and random vibration application', *J. vib. acoust. stress reliab. des. ASME*, **108**, 411–420 (1986).
44. M. N. Noori, M. Saffar, G. Ghantous, A. Guran, H. Davoodi and T. T. Baber, 'Equivalent linearization of a newly introduced general hysteretic model', in P. D. Spanos and C. A. Brebbia (eds), *Computational Stochastic Mechanics*, Computational Mechanics Publication, Boston, and Elsevier Applied Science, New York, 1991, pp. 279–291.
45. F. Alameddine and M. R. Ehsani, 'High-strength RC connections subjected to inelastic cyclic loading', *J. struct. eng. ASCE* **117**, 829–850 (1991).
46. K. Minami and M. Wakabayashi, 'Seismic resistance of reinforced concrete beam-and-column assemblages with emphasis on shear failure of columns', *Proc. 6th world conf. on earthquake engineering*, Vol. III, Sarita Prakashan, Meerut, India, 1977, pp. 3101–3106.
47. E. P. Popov and R. B. Pinkney, 'Cyclic yield reversal in steel building connections', *J. struct. div. ASCE* **95**(ST3), 327–353 (1969).
48. T. Yasuhiko, N. Noriyoshi, K. Ben and S. Toshio, 'Study on restoring force characteristics of X-steel braces', *Proc. 10th world conf. on earthquake engineering*, Balkema, Rotterdam, The Netherlands, 1992, pp. 2931–2936.
49. S. K. Kunnath, M. Mehrain and W. E. Gates, 'Seismic damage-control design of gypsum-roof diaphragms', *J. struct. eng. ASCE* **120**, 120–138 (1994).
50. M. Yasumura, 'Seismic behavior of arched frames and braced frames', *Proc. Int. Timber Engineering Conf.* Tokyo, Japan, Vol. 3, 1990, pp. 863–870.
51. M. A. Sozen, 'Hysteresis in structural elements', in W. D. Iwan (ed.), *Applied Mechanics in Earthquake Engineering*, ASME, New York, 1974, pp. 63–98.
52. G. C. Foliente, 'Stochastic dynamic response of wood structural systems'. *Ph.D. Thesis*, Virginia Polytechnic Institute and State University, Blacksburg, VA, 1993.